Electronic Supplementary Material (ESI) for Physical Chemistry Chemical Physics.

Supporting Information

Enhanced Moisture Stability of Cesium Lead Iodide Perovskite Solar cells- A First-Principles Molecular Dynamics Study

Dhana Lakshmi Busipalli, Kuan-Yu Lin, Santhanamoorthi Nachimuthu,* and Jyh-Chiang Jiang*

Department of Chemical Engineering, National Taiwan University of Science and Technology, Taipei 106, Taiwan, R.O.C.

* Corresponding authors: santhanamoorthi@gmail.com (SN), jcjiang@mail.ntust.edu.tw (JCJ)

Telephone: +886-2-27376653. Fax: +886-2-27376644.

Computational Details:

All the periodic DFT calculations were performed by using the Vienna Ab-initio Simulation Package (VASP). Here we considered the cubic $CH_3NH_3PbI_3$ perovskites for comparison. For $CH_3NH_3PbI_3$ perovskite, the optimized geometrical structure we choose from our previous study.[1] All calculations were performed by using the Generalized Gradient Approximation (GGA), as implemented by Perdew-Burke-Ernzerhof (PBE), was selected for the exchange-correlation functional. The projected augmented wave (PAW) method was employed to describe the electron-ion interaction. The convergence criterion was set to a 10^{-4} eV change in the energy during the geometry optimization iteration and the force on each atom is smaller than 0.01 eV/Å. The Brillion zone integrations were performed with 4 × 4 × 4 and 3 × 3 × 1 Monkhorst-Pack *k*-point grid for bulk and (100) surface calculations, respectively. We have added 15 Å for vacuum region for the simulation of the surface. A plane-wave basis set of 400 eV energy cut-off was adopted in all calculations. AIMD simulations were conducted under constant-volume and constant-temperature (NVT) conditions. Nose-Hoover thermostats were used and the temperature was set as 400 K. The total simulation time extended up of 10 ps and the time step of the integration of the dynamic equation was set to 1 fs. The Brillouin zone was sampled by using a Monkhorst-Pack grid with 2 × 2 × 1 for AIMD simulations.

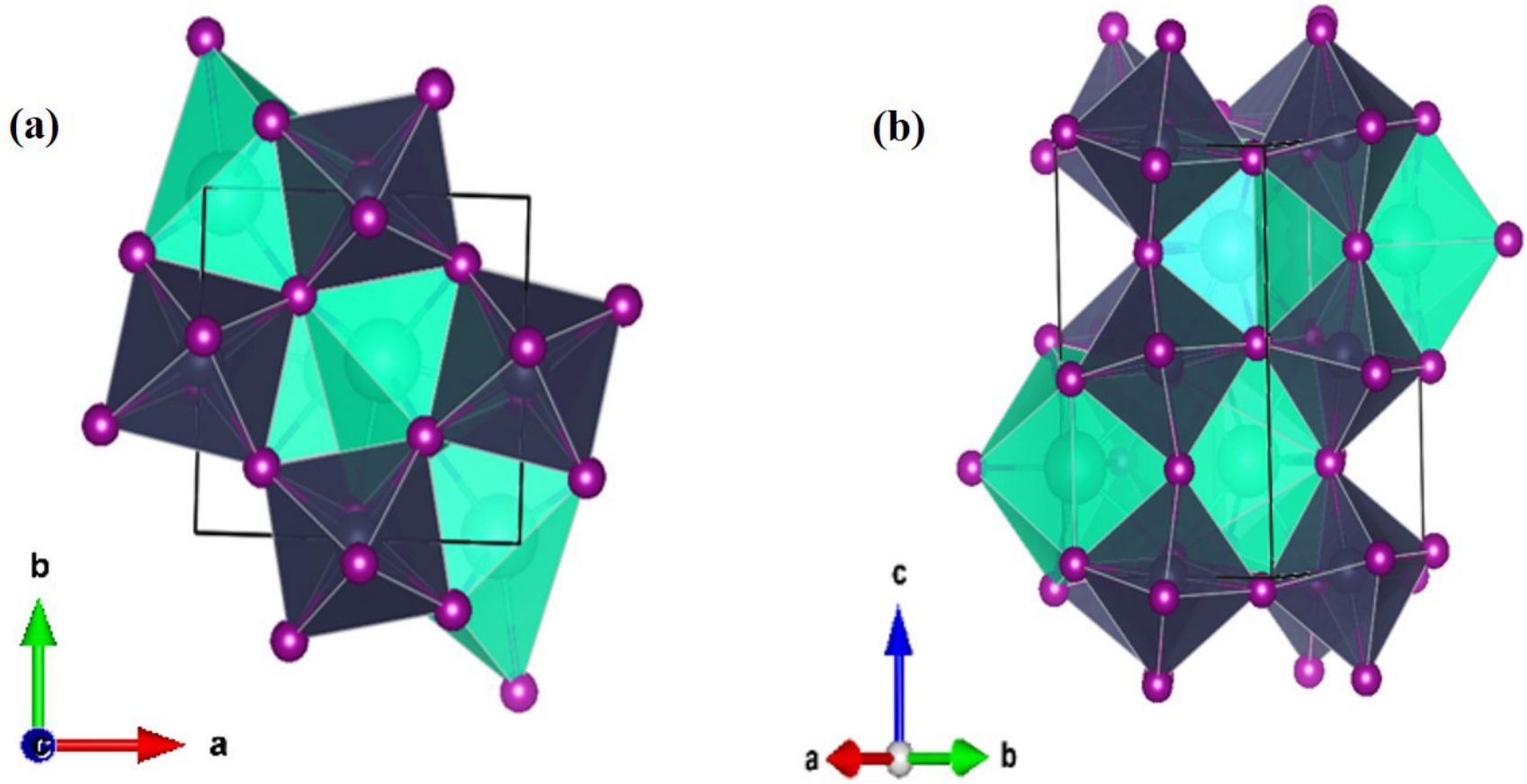

Fig. S1. The optimized geometrical structures of a) Top and b) Side views of γ-$CsPbI_3$ perovskite (Color coding: purple, I; gray, Pb; cyan, Cs).

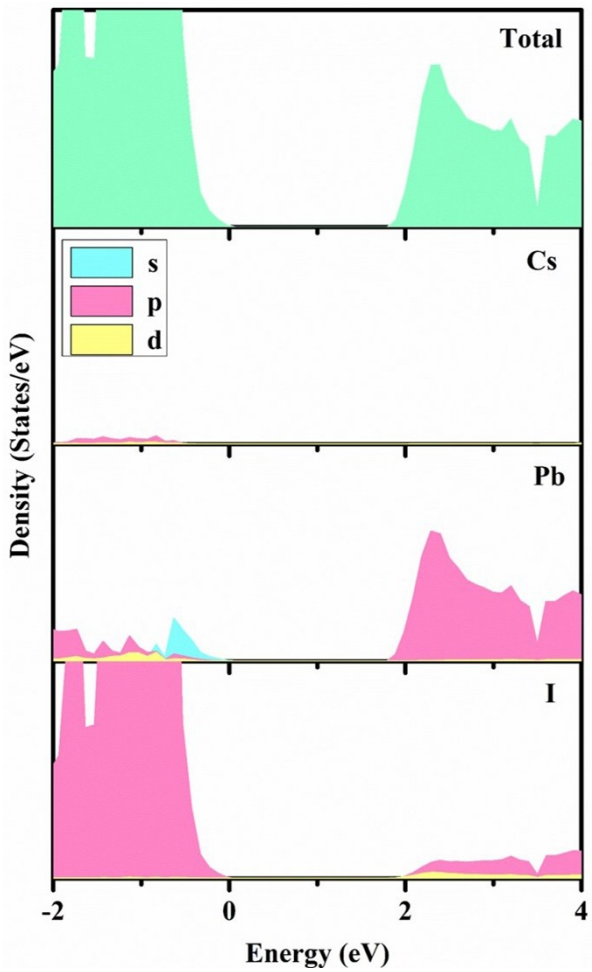

Fig. S2. The projected density of states (PDOS) of the γ-$CsPbI_3$ perovskite.

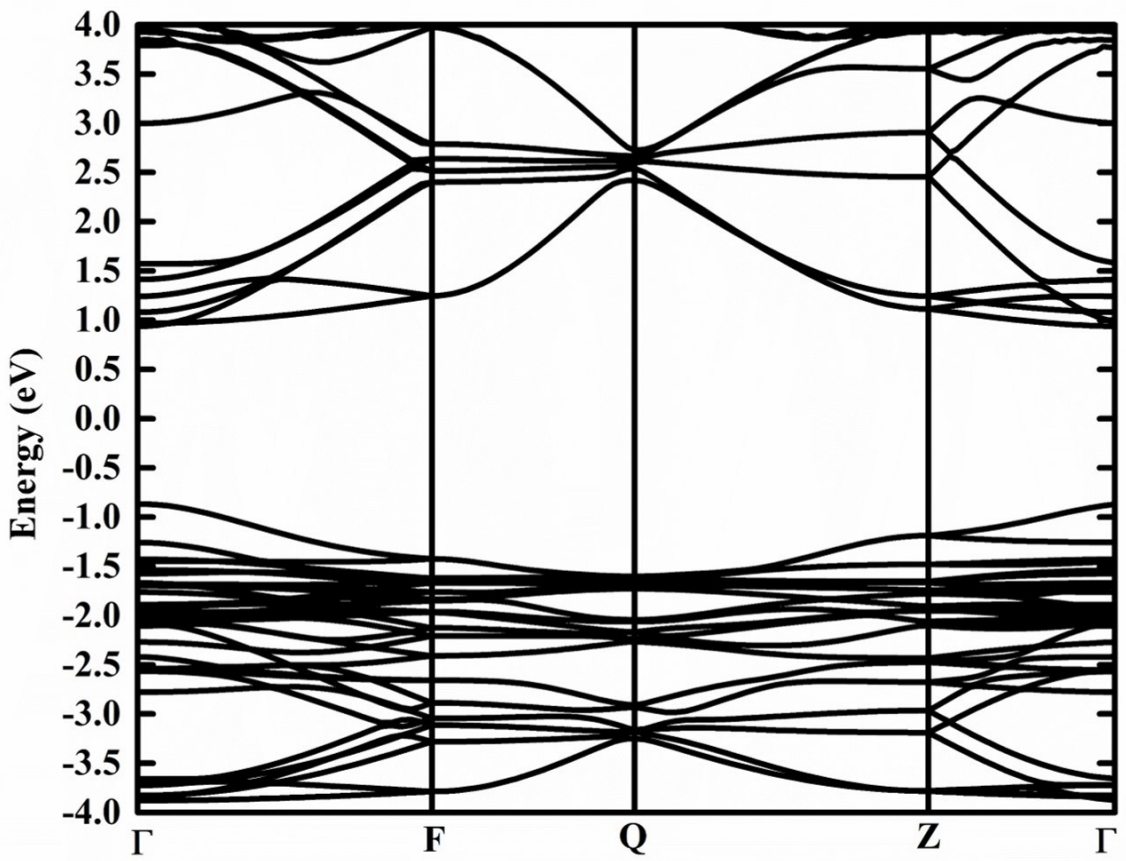

Fig. S3. Calculated band structure for the γ-$CsPbI_3$ perovskite.

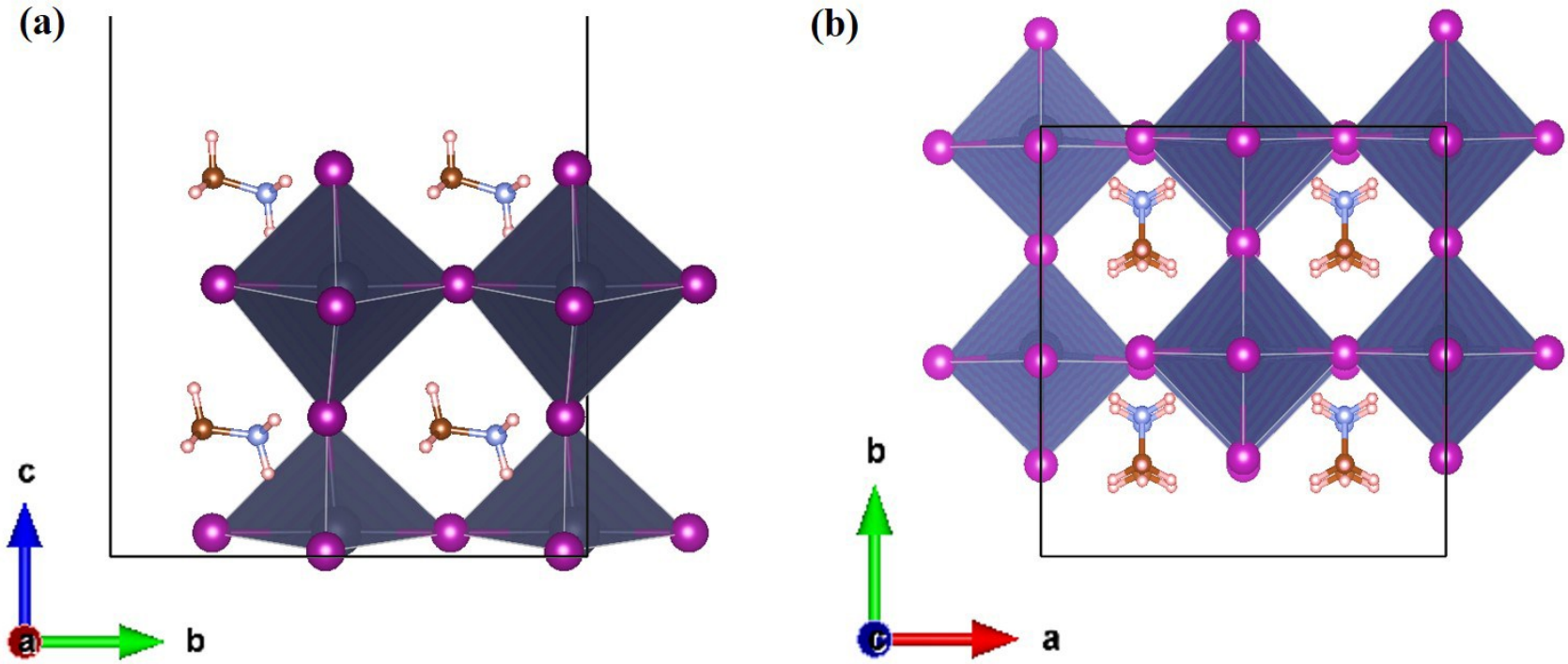

Fig. S4. Optimized slab model for CH_3NH_3I-terminated $CH_3NH_3PbI_3$ (100) surface (a) the side view, and (b) top view (Color coding: purple, I; gray, Pb; brown, C; blue, nitrogen, N; pink, H).

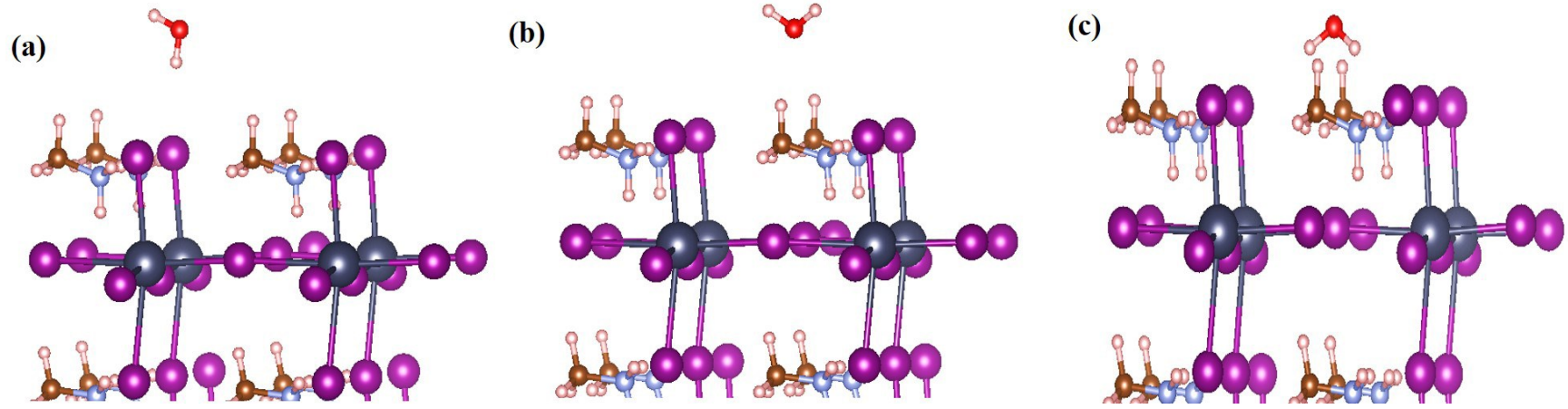

Fig. S5. The optimized geometrical structures of water adsorbed on (d) I-site, (e) CH_3NH_3-site and (f) hollow site of CH_3NH_3I-terminated $CH_3NH_3PbI_3$ (100) surfaces.

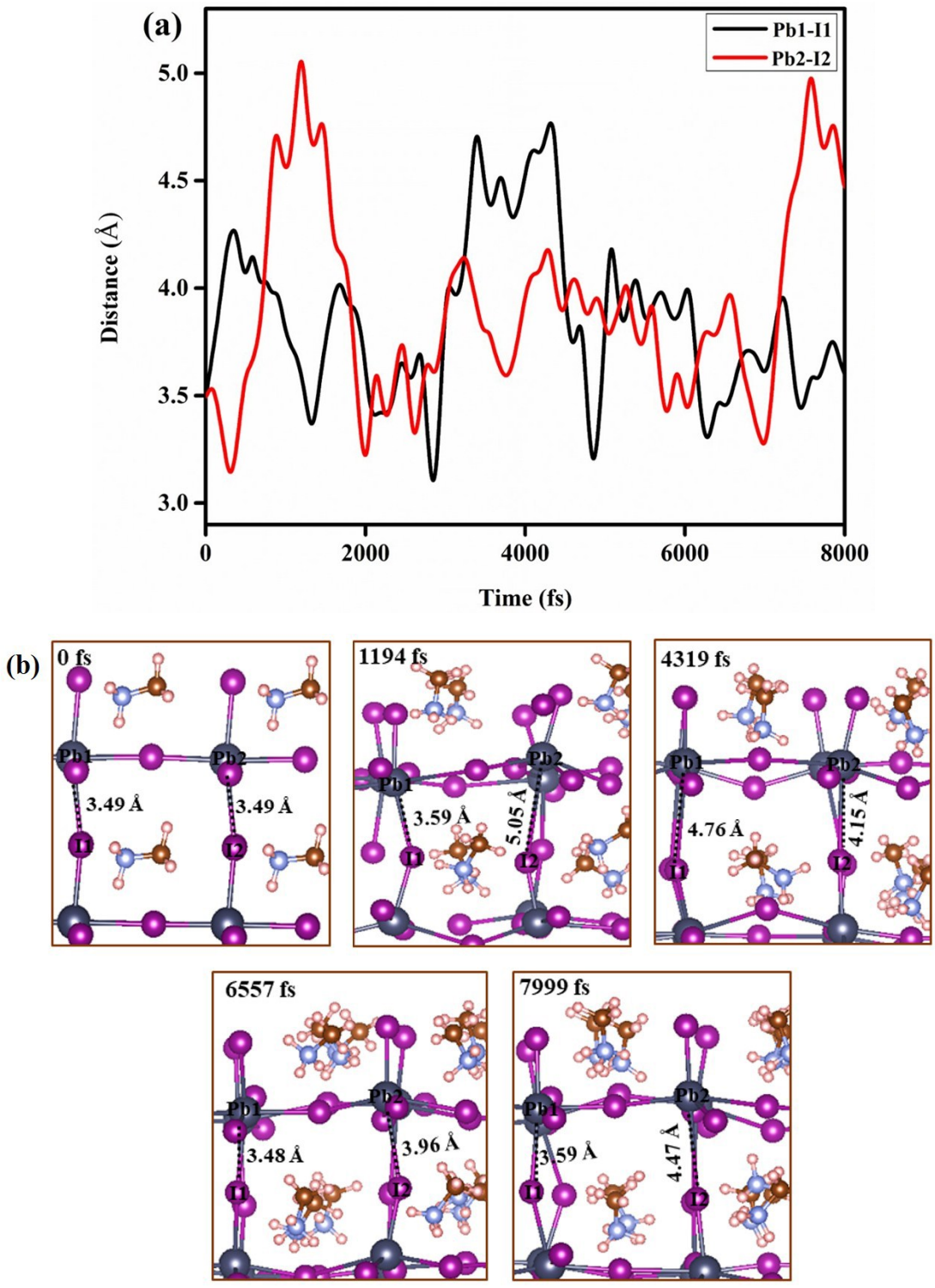

Fig. S6. (a) Evolution of the distances between Pb-I atoms with time variation, and (a) Side view of snapshots from the AIMD simulations of CH_3NH_3I-terminated surface at different simulation times.

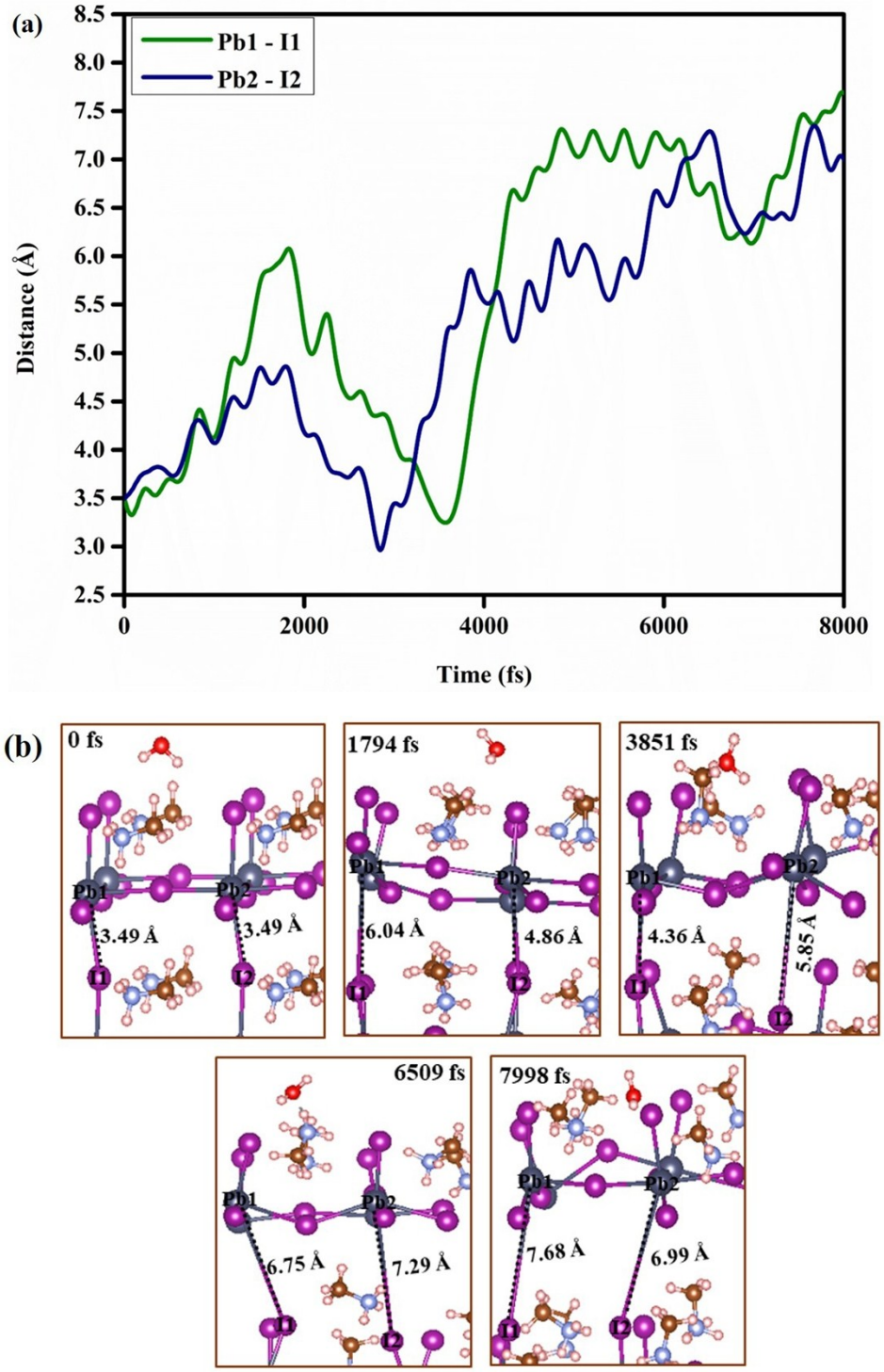

Fig. S7. (a) Evolution of the distances between Pb-I atoms with time variation, and (a) Side view of snapshots from the AIMD simulations with the H_2O molecule on the CH_3NH_3I-terminated surface at different simulation times.

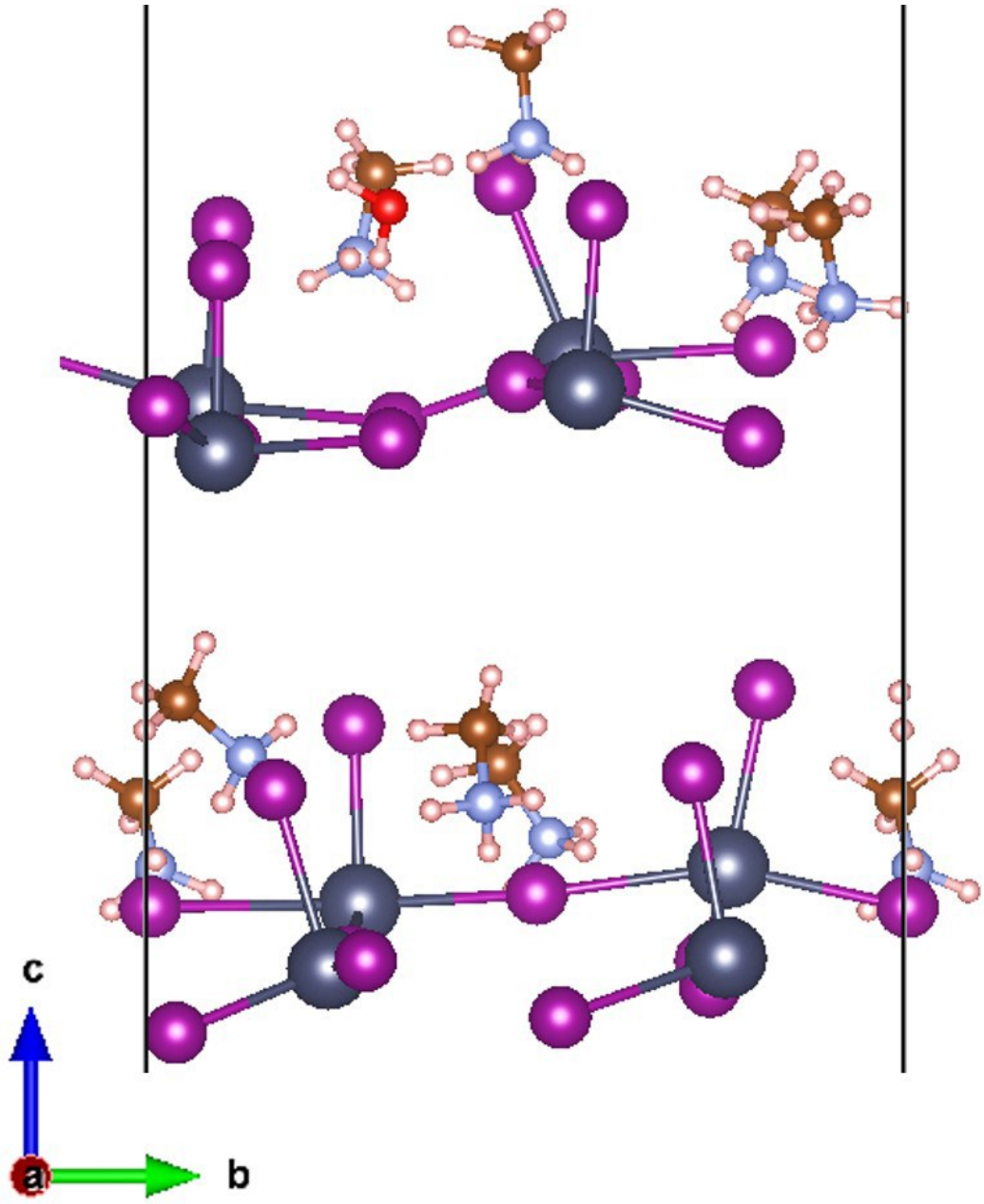

Fig. S8. The configuration of the CH_3NH_3I-terminated $CH_3NH_3PbI_3$ (100) surface at the end of simulation time.

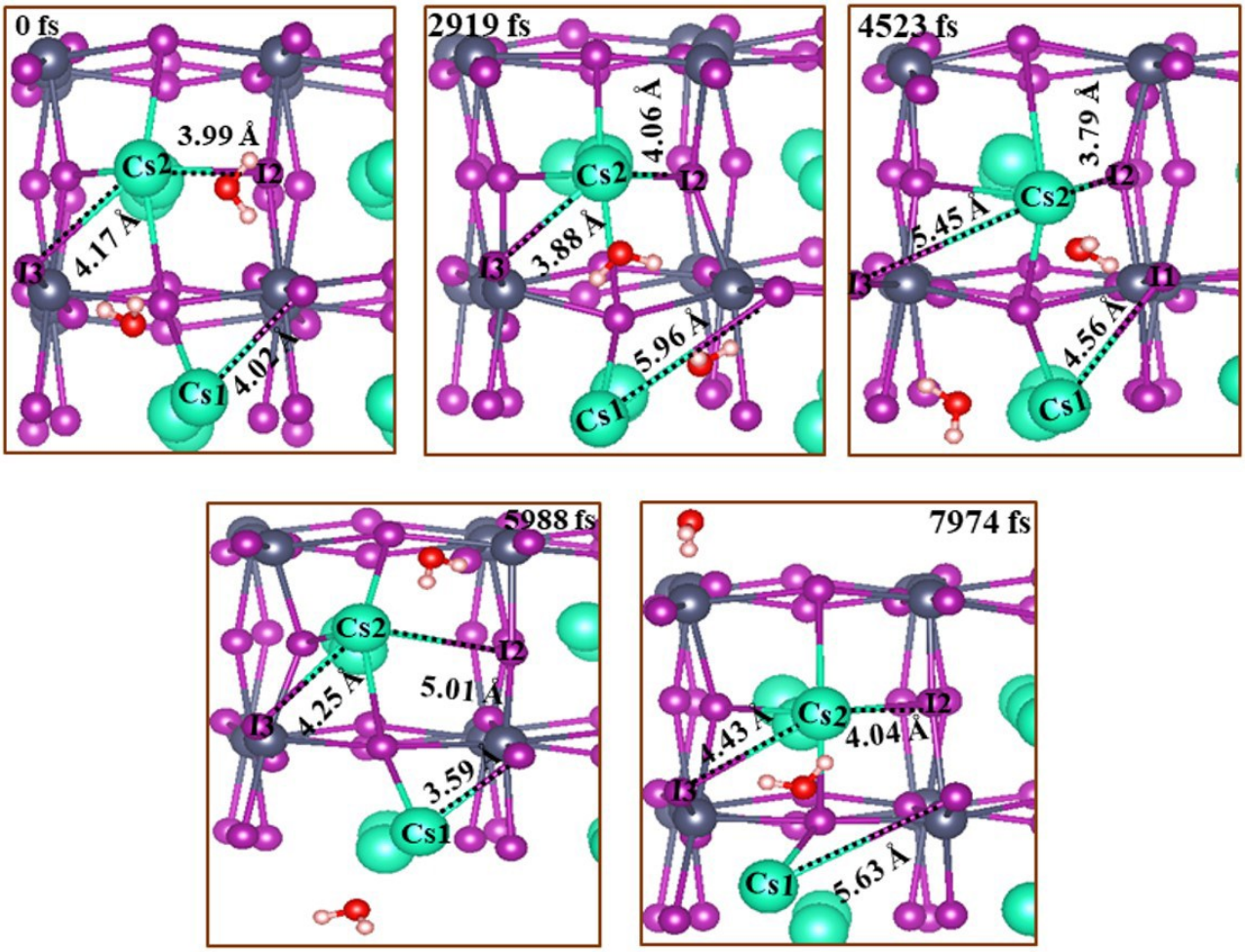

Fig. S9. Top view of snapshots from the AIMD simulations with two water molecules on the CsI-terminated γ-$CsPbI_3$ (220) surface at different simulation times.

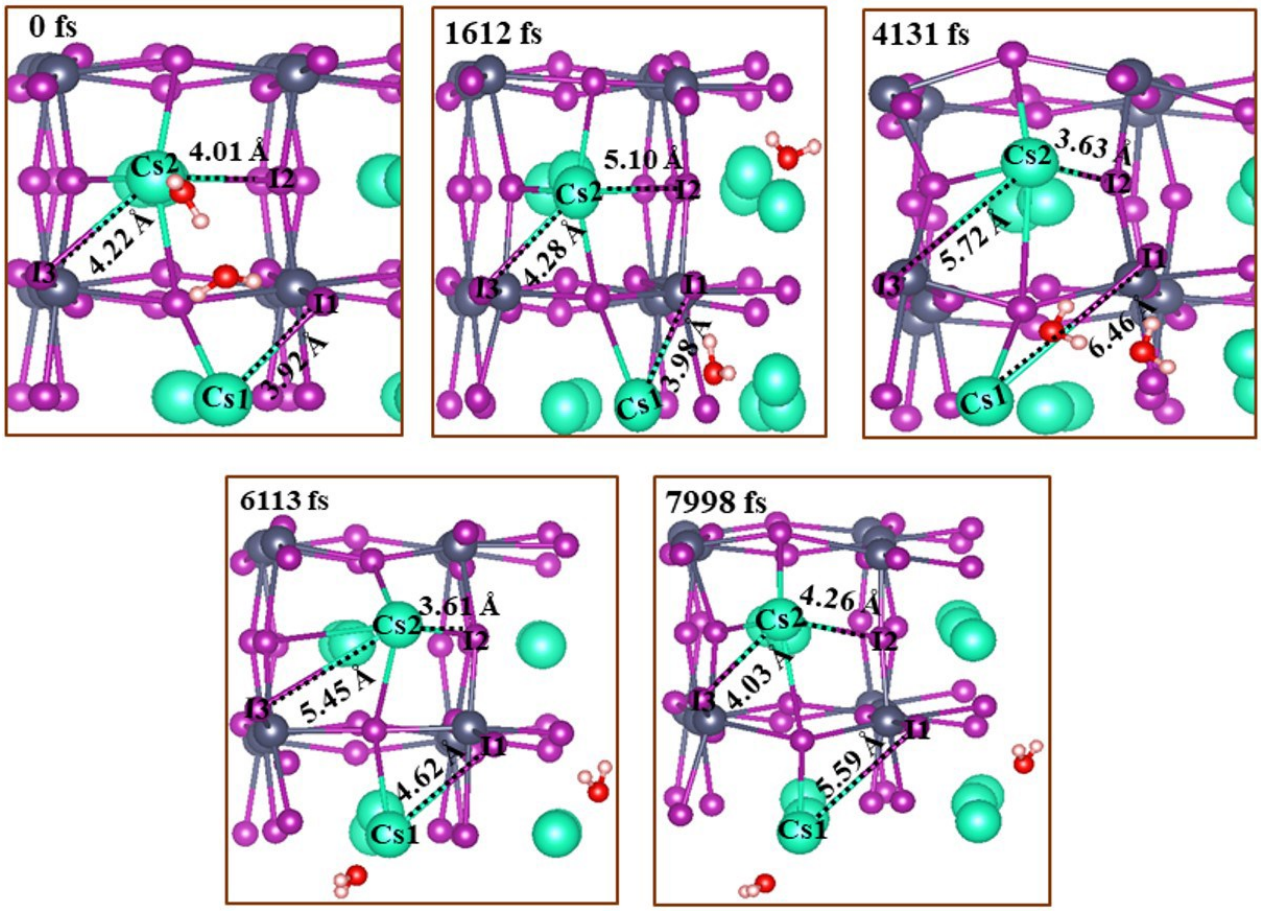

Fig. S10. Top view of snapshots from the AIMD simulations with the water dimer on the CsI-terminated γ-$CsPbI_3$ (220) surface at different simulation times.

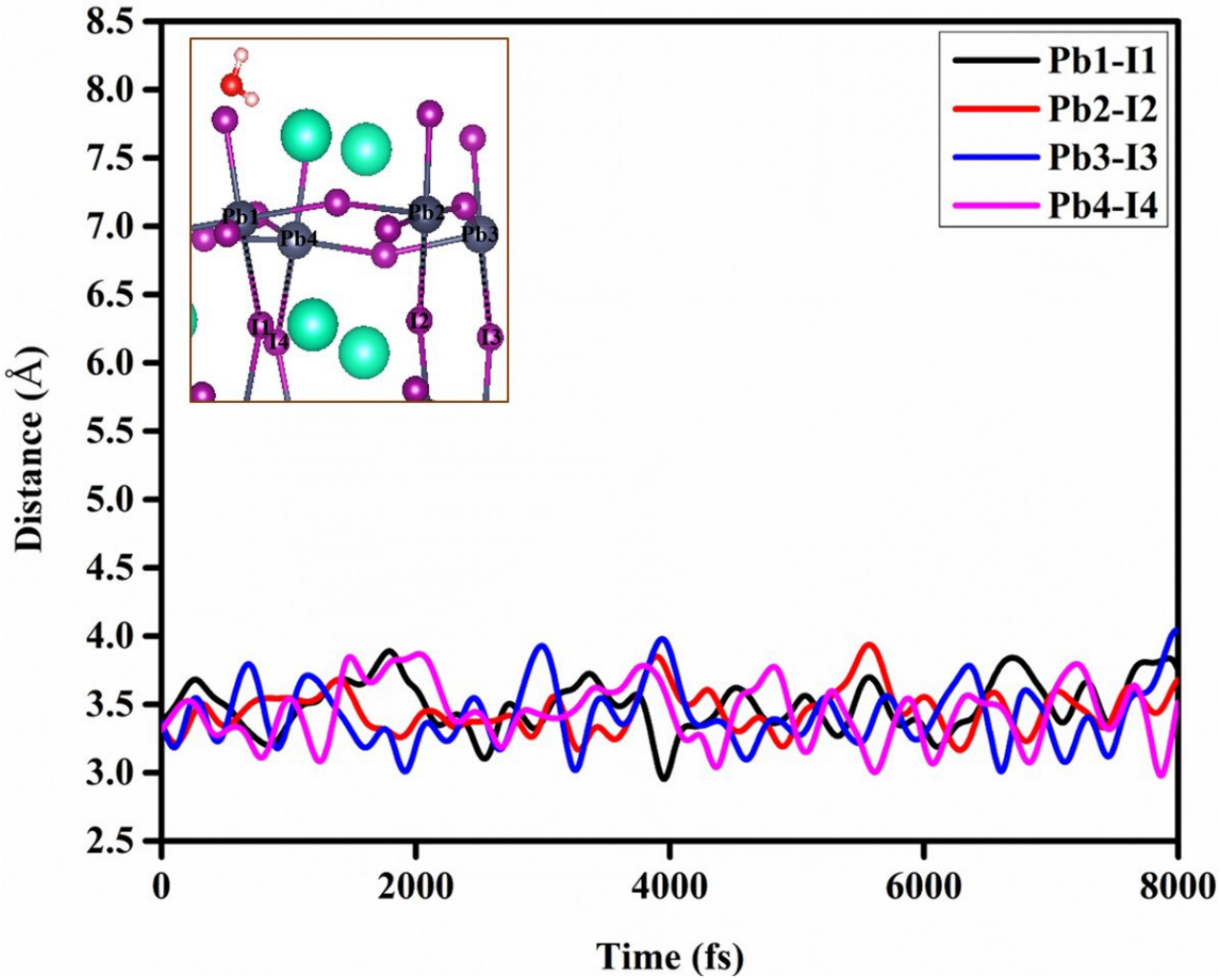

Fig. S11. Evolution of the distances between the lead and the iodine atoms for the water monomer adsorbed on the CsI-terminated $CsPbI_3$ (220) surface at different simulation times.

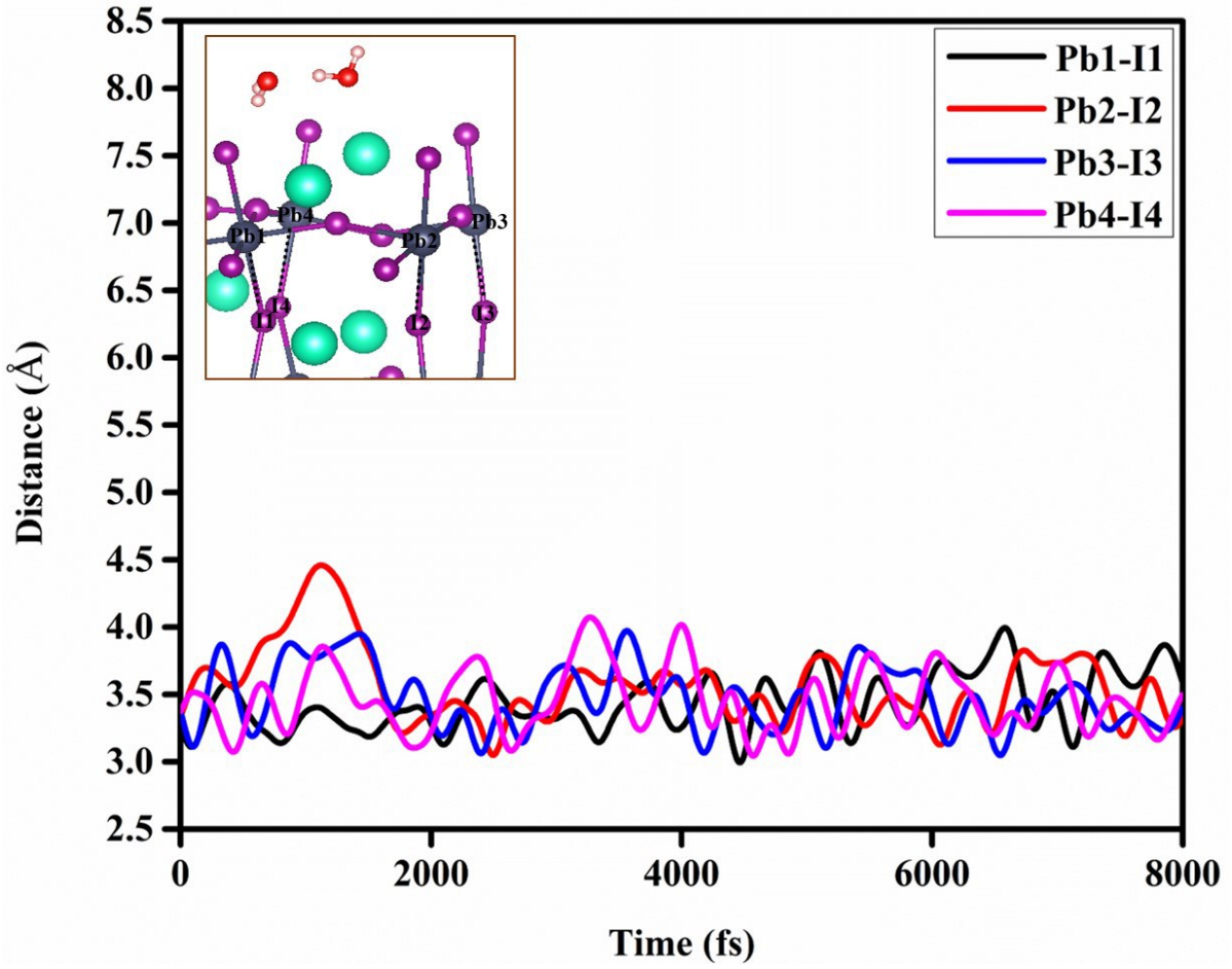

Fig. S12. Evolution of the distances between the lead and the iodine atoms for the water dimer adsorbed on the CsI-terminated $CsPbI_3$ (220) surface at different simulation times.

Table S1. The calculated lattice parameters (in Å) of the γ-$CsPbI_3$ structure using different functionals along with the experimental values.

	a	**b**	**c**
PBE	9.0674 (2.4%)	8.7576 (2.1%)	12.6777 (1.6%)
PW91	9.0697 (2.4%)	8.7405 (1.9%)	12.6741 (1.6%)
RPBE	9.2156 (4.1%)	9.0539 (5.6%)	13.0032 (4.3%)
Exp.[2]	8.8561	8.5766	12.4722

Data in parentheses refer to the percentage of deviation with respect to the experimental values.

Table S2. The calculated lattice parameters (in Å) of the γ-$CsPbI_3$ structure using PBE functional with different cutoff energies along with the experimental values.

Cutoff energy (eV)	a	b	c
300	9.0602 (2.3%)	8.7464 (2.0%)	12.6714 (1.6%)
400	9.0674 (2.4%)	8.7576 (2.1%)	12.6777 (1.6%)
500	9.0694 (2.4%)	8.7480 (2.0%)	12.6813 (1.7%)
600	9.0625 (2.3%)	8.7525 (2.1%)	12.6775 (1.6%)
Exp.[2]	8.8561	8.5766	12.4722

Data in parentheses refer to the percentage of deviation with respect to the experimental values.

Table S3. The calculated band gaps (in eV) of $CsPbI_3$ Perovskite, compared with available experimental results.

$CsPbI_3$	**Calculated Band gap (eV)**	**Experimental Band gap (eV)**
δ - phase	2.76	2.82[3, 4]
γ - phase	1.86	1.69[5]
α - phase	1.53	1.73[6, 7]

γ-$CsPbI_3$ (220)		**δ -$CsPbI_3$ (212)**	
Surface Termination	Surface Energy (eV/Å^2)	Surface Termination	Surface Energy (eV/Å^2)
I-termination	0.073	I-termination	0.048
Cs-termination	0.038	I-rich termination	0.062
PbI_2-termination	0.030	Pb-termination	0.059
CsI-termination	0.027	Cs-termination	0.065
PbI_2-defective termination	0.066	CsI-termination 1	0.057
PbI_2-rich defective termination	0.054	CsI-termination 2	0.064
CsI-defective termination	0.032	PbI_2-termination	0.051
I-rich termination	0.106	PbI_2-rich termination	0.056

Table S4. The calculated surface energies for the different terminations of γ-phase $CsPbI_3$ (220) and δ-phase $CsPbI_3$(212) surfaces.

Table S5. The calculated structural parameters (interatomic bond lengths and angle) of water molecule adsorbed on the γ-$CsPbI_3$(220) surface.

Site	Structural Parameters		
	$d_{O\text{-}Ha}$ (Å)	$d_{O\text{-}Hb}$ (Å)	∠ H-O-H(degree)
Cs-site	0.973	0.974	104.70
I-site	0.981	0.973	104.67
Hollow site	0.980	0.973	104.25

Reference:

1. D. L. Busipalli, S. Nachimuthu and J. C. Jiang, *J. Chin. Chem. Soc.*, 2019, **66**, 575-582.
2. R. J. Sutton, M. R. Filip, A. A. Haghighirad, N. Sakai, B. Wenger, F. Giustino and H. J. Snaith, *ACS Energy Lett.*, 2018, **3**, 1787-1794.
3. G. E. Eperon, G. M. Paterno, R. J. Sutton, A. Zampetti, A. A. Haghighirad, F. Cacialli and H. J. Snaith, *J. Mater. Chem. A*, 2015, **3**, 19688-19695.
4. B. Y. Zhao, S. F. Jin, S. Huang, N. Liu, J. Y. Ma, D. J. Xue, Q. W. Han, J. Ding, Q. Q. Ge, Y. Q. Feng and J. S. Hu, *J. Am. Chem. Soc.*, 2018, **140**, 11716-11725.
5. K. Wang, Z. W. Jin, L. Liang, H. Bian, D. L. Bai, H. R. Wang, J. R. Zhang, Q. Wang and S. Z. Liu, *Nat. Commun*, 2018, **9**, 4544.
6. A. Swarnkar, A. R. Marshall, E. M. Sanehira, B. D. Chernomordik, D. T. Moore, J. A. Christians, T. Chakrabarti and J. M. Luther, *Science*, 2016, **354**, 92-95.
7. C. C. Stoumpos, C. D. Malliakas and M. G. Kanatzidis, *lnorg. Chem.*, 2013, **52**, 9019-9038.